ELSEVIER

Chemical Engineering Journal 144 (2008) 175–180

Chemical Engineering Journal

www.elsevier.com/locate/cej

Promoting effect of copper on the catalytic activity of MnO_x–CeO_2 mixed oxide for complete oxidation of benzene

Xingfu Tang, Yide Xu, Wenjie Shen *

State Key Laboratory of Catalysis, Dalian Institute of Chemical Physics, Chinese Academy of Sciences, Dalian 116023, China

Received 14 June 2006; received in revised form 19 January 2007; accepted 13 January 2008

Abstract

The promoting effect of copper on the catalytic activity of MnO_x–CeO_2 for complete oxidation of benzene was investigated. The results showed that the addition of copper could significantly improve the catalytic activity of the mixed oxide and the complete conversion of benzene was achieved at 523 K. Structural analysis by X-ray powder diffraction (XRD) and H_2-temperature-programmed reduction (H_2-TPR) measurements indicated that the copper species was highly dispersed on the surface of the mixed oxide, which greatly promoted the redox properties of the catalyst leading to the at low temperatures. X-ray photoelectron spectra (XPS) and FTIR characterizations of the Cu/MnO_x–CeO_2 catalyst further revealed that the addition of copper significantly increased the generation of surface O_β species and also created more active sites for benzene adsorption.

Keywords: MnO_x–CeO_2; Cu/MnO_x–CeO_2; Promotion effect; Benzene oxidation

1. Introduction

Benzene is a hazardous volatile organic compound presenting in various industries such as chemical, petrochemical, paint and coating and steel manufacture. Catalytic oxidation is regarded as one of the most promising routes for the effective removal of benzene in lower concentrations. Supported noble metal catalysts, typically Pd, have been generally preferred for the complete oxidation of benzene due to the higher activity [1–5]. Complete oxidation of benzene was achieved at 553 K on Pd–V_2O_5/Al_2O_3 catalysts [2]. Supported Pt or Pt–Pd bimetal catalysts also showed promising activities for complete oxidation of benzene, and the temperatures required for total conversion of benzene were 483–523 K [3,6].

Quite recently, supported gold–vanadium catalysts were reported to be effective for complete oxidation of benzene, and the nature of the support was found to play a key role in the activities [7,8]. Noticeably, ceria could act as efficient support or promoter and 100% conversion of benzene was reached at 473–573 K [7–9]. Supported copper were reported as promising catalysts for complete oxidation of benzene and other contaminants. Cu/Al_2O_3 was found to be the most active catalyst among the transition metals for the complete oxidation of benzene, toluene and xylene [10]. CuO/CeO_2 catalyst was observed to show better catalytic performance for the complete oxidation of benzene, toluene and *p*-xylene than that of CuO/Al_2O_3 catalyst [11]. Indeed, ceria-supported copper catalysts were also reported to be effective for preferential oxidation of CO [12,13] and wet oxidation of phenol [14,15]. The role of copper was attributed to enhance the oxygen vacancies on the surface of ceria, which are responsible for the high catalytic activity [13–15].

MnO_x–CeO_2 mixed oxides could exhibit much better redox properties than ceria alone [16,17], and we recently demonstrated that MnO_x–CeO_2 mixed oxides were highly active for the complete oxidation of formaldehyde at low temperatures [18]. The aim of this work was to study of the effect of copper promotion on the MnO_x–CeO_2 mixed oxide for the complete oxidation of benzene. The structural features of the MnO_x–CeO_2 mixed oxide and the Cu/MnO_x–CeO_2 catalyst was characterized by XRD, H_2-TPR and XPS techniques.

2. Experimental

2.1. Catalyst preparation

The MnO_x–CeO_2 mixed oxide (Mn/(Mn + Ce) = 0.5, molar ratio) was prepared by a modified co-precipitation method as

* Corresponding author. Tel.: +86 411 84379085; fax: +86 411 84694447.
E-mail address: shen98@dicp.ac.cn (W. Shen).

1385-8947/$ – see front matter © 2008 Elsevier B.V. All rights reserved.
doi:10.1016/j.cej.2008.01.016

described elsewhere [18]. Briefly, 2 M KOH aqueous solution was slowly added to an aqueous solution containing $Mn(NO_3)_2{\cdot}6H_2O$, $KMnO_4$ and $(NH_4)_2Ce(NO_3)_6$ with a molar ratio of 3:2:5 at 323 K until the pH value of the mixture reached 10.5 under vigorous stirring. The precipitate was further aged at 323 K for 2 h in the mother liquid. After filtering and washing with distilled water, the obtained solid was dried at 383 K for 12 h and calcined at 773 K for 6 h in air.

The Cu/MnO_x–CeO_2 catalyst was prepared by a deposition precipitation method. The MnO_x–CeO_2 powder was dispersed in the aqueous solution containing known amount of $Cu(NO_3)_2{\cdot}3H_2O$. Then, 0.25 M KOH aqueous solution was slowly added at 323 K until the pH value of the mixed solution reached 10.5 under stirring. The mixture was further aged at 323 K for 2 h in the mother liquid under stirring, during which copper hydroxide was exclusively precipitated on the surface of MnO_x–CeO_2. After filtration, the resulting solid was washed with distilled water, dried at 383 K for 12 h and finally calcined at 773 K for 6 h in air. The actual loading of copper was determined to be 2.54 wt.% by elemental analysis performed with Inductively Coupled Plasma Atomic Emission Spectroscopy (ICP-AES) on a Plasam-Spec-I spectrometer.

2.2. Catalyst characterization

The BET surface areas of the samples were measured by N_2 adsorption–desorption isotherms at 77 K using a Micromeritics ASAP 2000 instrument. Prior to the measurements, the samples were degassed in vacuum at 573 K for 2 h.

X-ray powder diffraction (XRD) patterns were recorded with a D/Max-2500/PC powder diffractometer (Rigaku, Japan) operated at 40 kV and 250 mA, using nickel-filtered Cu Kα ($\lambda = 0.15418$ nm) radiation. The average crystallite sizes of the cubic ceria phase were calculated according to the Scherrer equation, and the lattice parameters were calculated according to the Cohen procedure [19].

H_2-temperature-programmed reduction (H_2-TPR) measurements were carried out on a CHEMBET 3000 adsorption instrument (Quantachrome, USA) equipped with a TCD detector. Thirty milligrams of sample was loaded and pretreated with He at 573 K for 1 h to remove the adsorbed carbonates and hydrates. After cooling down to room temperature and introducing the reducing agent of 5% H_2/Ar (50 ml/min), the temperature was then programmed to rise at a heating rate of 10 K/min.

X-ray photoelectron spectra (XPS) were recorded on a KROTAS AMICAS spectrometer (Shimadzu, Japan) with a magnesium anode for Kα ($h\nu = 1253.6$ eV) radiation. The samples were pretreated in a chamber at 2×10^{-8} Pa at 523 K for 1 h to remove the adsorbed carbonates and hydrates. The charging effect was corrected by adjusting the binding energy of C 1s to 284.6 eV. The O 1s spectrum was deconvoluted by using the XPSPEAK program.

2.3. FTIR characterization

FTIR spectra of adsorbed benzene were measured with a Vector 22 spectrometer (Bruker, Germany) equipped with a DTGS detector. The self-supported wafer (around 15 mg and 1.3 cm in diameter) was loaded into an IR cell with ZnSe windows. The wafer was first treated with He (99.999%, 30 ml/min) at 523 K for 1 h and cooled to a given temperature, then exposed to the flow of 200 ppm benzene in 20.0% O_2/He (ca. 30 ml/min) for 30 min, and flushed with He again for 30 min at the same temperature. FTIR spectra were recorded by accumulating 64 scans at a spectra resolution of 4 cm^{-1}. The background spectrum was recorded prior to the introduction of benzene and subtracted from the sample spectrum.

2.4. Activity measurement

Complete oxidation of benzene was performed in a fixed-bed reactor under atmospheric pressure in the temperature range of 423–648 K. Two hundred milligrams of catalyst (40–60 mesh) was sandwiched by quartz wool layers in a quartz tube reactor. The feed gas was composed of 200 ppm benzene and 20.0 vol.% oxygen balanced with helium. The total flow rate was 100 ml/min, corresponding to a gas hourly space velocity (GHSV) of 30,000 ml/(g_{cat} h). The effluents from the reactor were analyzed by an on-line HP 6890 gas chromatograph equipped with TCD and FID detectors. A Haysep D packing column was used to detect the CO, CO_2 and O_2, and an Innowax capillary column was employed to separate oxygenates and hydrocarbons. In typical runs, the reaction data were taken after benzene oxidation was performed for 3 h in order to achieve the steady state.

3. Results and discussion

3.1. Physical and chemical properties of the catalysts

Table 1 lists the BET surfaces, and particle sizes and lattice parameters of the samples. Clearly, the specific surface area of the MnO_x–CeO_2 support was measured to be 124 m^2/g, which was slightly decreased to 118 m^2/g by the loading of 2.54 wt.% copper. Fig. 1 shows the XRD patterns of the MnO_x–CeO_2 support and the Cu/MnO_x–CeO_2 catalyst. The mixed oxide only showed typical diffractions of CeO_2 with cubic fluorite structure, and no diffractions of manganese oxides could be observed. This is in good consistent with the recent report that the diffraction patterns of MnO_x–CeO_2 mixed oxides at $Mn/(Mn + Ce) \geq 0.75$

Table 1
Physical and chemical properties of the MnO_x–CeO_2 and Cu/MnO_x–CeO_2 catalysts

Sample	Cu content (wt.%)	BET surface area (m^2/g)	Particle size (nm)	Lattice parameter (nm)
MnO_x–CeO_2	–	124	3.2	0.5378
Cu/MnO_x–CeO_2	2.54	118	3.2	0.5378

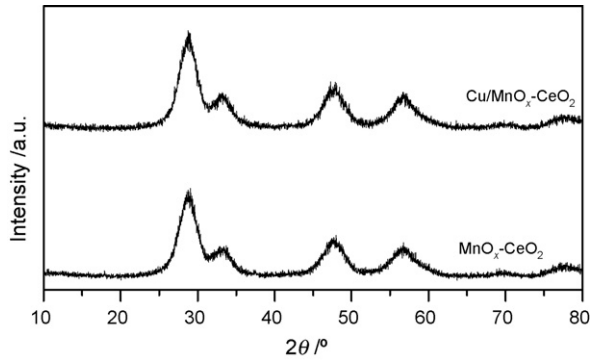

Fig. 1. XRD patterns of the MnO_x–CeO_2 support and the Cu/MnO_x–CeO_2 catalyst.

(molar ratio) showed crystallization of Mn_2O_3, whereas those at Mn/(Mn + Ce) ≤ 0.5 consisted of only broad peaks attributed to CeO_2 due to the formation of solid solution between MnO_x and CeO_2 [20]. For the current MnO_x–CeO_2 mixed oxide, the Mn/(Mn + Ce) ratio was designed to be 0.5, and it was highly possible to form solid solution during the precipitation and calcination processes, as confirmed by our recent report [18]. The Cu/MnO_x–CeO_2 catalyst showed similar XRD diffractions as the corresponding support, and no diffraction peaks due to Cu species could be observed. This indicated that the copper species were highly dispersed on the surface of the MnO_x–CeO_2 support. The average particle size and the lattice parameter of ceria in the Cu/MnO_x–CeO_2 catalyst were calculated to be 3.3 and 0.5378 nm, which remained essentially unchanged after the deposition of copper, as shown in Table 1.

Fig. 2 shows the H_2-TPR profiles of CeO_2, CuO, MnO_x–CeO_2 and Cu/MnO_x–CeO_2 samples. The reductions of surface and bulk oxygen of CeO_2, depending on the surface areas, usually occurred at approximately 770 and 1100 K, respectively [21]. For the current CeO_2, only a weak and broad reduction peak was observed at about 850 K with a H_2 consumption of 726 μmol/g. This phenomenon corresponded to the reduction of surface oxygen of ceria. CuO was stoichiometrically reduced into metallic copper at 631 K. The MnO_x–CeO_2 exhibited two intensive reduction peaks at 644 and 703 K, respectively, with the total hydrogen consumption of 4191 μmol/g. As we previously reported [18], the low temperature reduction could be assigned to the reduction of MnO_2 to Mn_3O_4 and the high temperature reduction represented the combined reduction of Mn_3O_4 to MnO and surface oxygen of ceria. The Cu/MnO_x–CeO_2 catalyst showed an intensive reduction peak at about 634 K, with a broad shoulder peak at about 576 K. Obviously, the presence of copper significantly shifted the high-temperature reduction peak to lower temperature regions, indicating the occurrence of metal-support interaction between copper and MnO_x–CeO_2. This improvement was often interpreted in terms of the activation and spillover of hydrogen from the initially reduced copper to the manganese and cerium oxides [22]. Thus, it can be deduced that the broad peak at 576 K in the H_2-TPR profile of the Cu/MnO_x–CeO_2 catalyst corresponded to the reduction of MnO_2 to Mn_3O_4, and the high-temperature reduction peak at 634 K represented the reductions of CuO, surface CeO_2 and Mn_3O_4. The amount of hydrogen consumption was calculated to be 4377 μmol/g, further confirming the combined reduction of copper oxide and manganese–cerium oxides.

Fig. 3 shows the XP spectra of O 1s in MnO_x–CeO_2 mixed oxide and the Cu/MnO_x–CeO_2 catalyst. Two surface oxygen species could be distinguished. The lower binding energy at 529.2 eV could be ascribed to the lattice oxygen (O^{2-}) (hereafter denoted as O_α) [18,23,24], and the higher binding energy at 531.4 eV was assigned to the defective oxides, or the surface oxygen ions with low coordination (hereafter denoted as

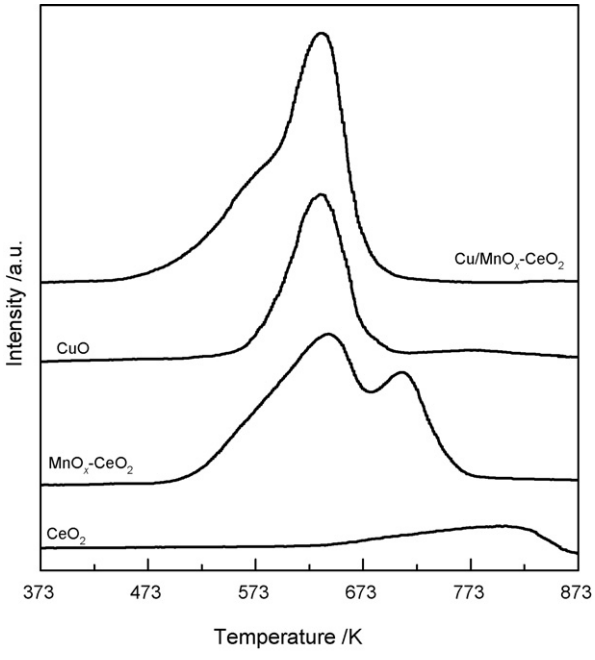

Fig. 2. H_2-TPR profiles of CeO_2, CuO, MnO_x–CeO_2 and Cu/MnO_x–CeO_2 samples.

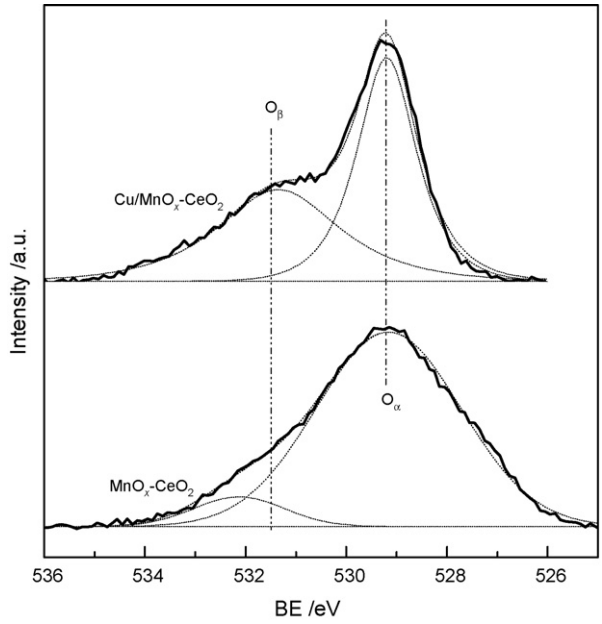

Fig. 3. XP spectra of O 1s in the MnO_x–CeO_2 and Cu/MnO_x–CeO_2 catalysts.

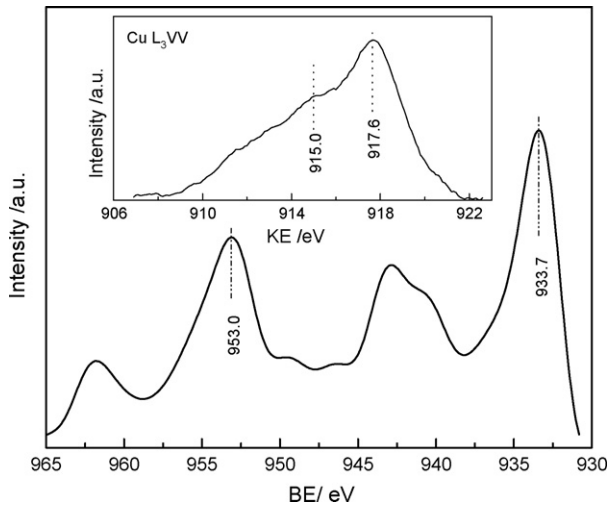

Fig. 4. XP spectrum of Cu 2p and Cu Auger spectra of the Cu/MnO_x–CeO_2 catalyst.

O_β) [16,25,26]. The relative concentration of O_β calculated from the XP spectra was 46% for the Cu/MnO_x–CeO_2 catalyst, which was much higher than that of the MnO_x–CeO_2 mixed oxide support (9%) [18]. Therefore, the addition of copper to MnO_x–CeO_2 mixed oxide caused the generation of defective oxides and/or surface oxygen species with low coordination, through the interaction between copper and MnO_x–CeO_2 mixed oxide.

Fig. 4 illustrated XP spectrum of Cu 2p and Cu Auger spectra of the Cu/MnO_x–CeO_2 catalyst. The main peak of Cu $2p_{3/2}$ at 933.7 eV together with the shake-up satellites was apparently the characteristics of Cu^{2+}. The spectra of Cu L3VV Auger can be resolved into two peaks at about 917.6 and 915.0 eV. The kinetic energy at 917.6 eV also corresponded to the value expected for CuO. Therefore, the copper species in the Cu/MnO_x–CeO_2 catalyst could be comprehensively assigned to CuO [22,27], while the minor presence of Cu+ at 915.0 eV was mainly due to the slight photoreduction of CuO in the spectrometer.

3.2. FTIR study

Fig. 5 shows the IR spectra of adsorbed benzene on MnO_x–CeO_2 and Cu/MnO_x–CeO_2 catalyst together with that of gas-phase benzene. Adsorbed benzene on the Cu/MnO_x–CeO_2 catalyst gave one primary pair of bands at 1977 and 1833 cm^{-1}, which may be assigned to out-of-plane vibration of C–H band of benzene molecules strongly interacting with the metal ions of the catalyst [28]. Very weak bands at 1883 and 2049 cm^{-1} were also discerned, corresponding to that of benzene molecules which interacted with the surface oxygen atoms of the catalyst [28]. Apparently, most of the adsorbed benzene located on the surface of the metal cations and the interaction of benzene with the surface oxygen can be negligible. Noticeably, two bands at 1178 and 1148 cm^{-1}, corresponding to the in-plane bending of C–H (βC–H), could be clearly observed, which originated from the strong interactions of benzene with the metal ions of the catalysts since these two bands were absent in the IR spectrum of gas-phase benzene under the same conditions. Similar IR spectra of the adsorbed benzene on the MnO_x–CeO_2 support were also observed, but the intensities of the spectra were remarkably decreased, suggesting that the addition of the copper species to the MnO_x–CeO_2 mixed oxide significantly increased the amount of adsorbed benzene.

The C–C stretching vibration band at 1479 cm^{-1} was observed over MnO_x–CeO_2 and Cu/MnO_x–CeO_2 catalyst, similar to the previous findings [29]. It becomes weaker with increasing the temperature, and almost disappeared when the temperature reached to 473 K. However, it could be seen that the intensity of the adsorbed benzene on the Cu/MnO_x–CeO_2 catalyst was much stronger than that over the MnO_x–CeO_2 support, indicating that the addition of copper enhanced the affinity of

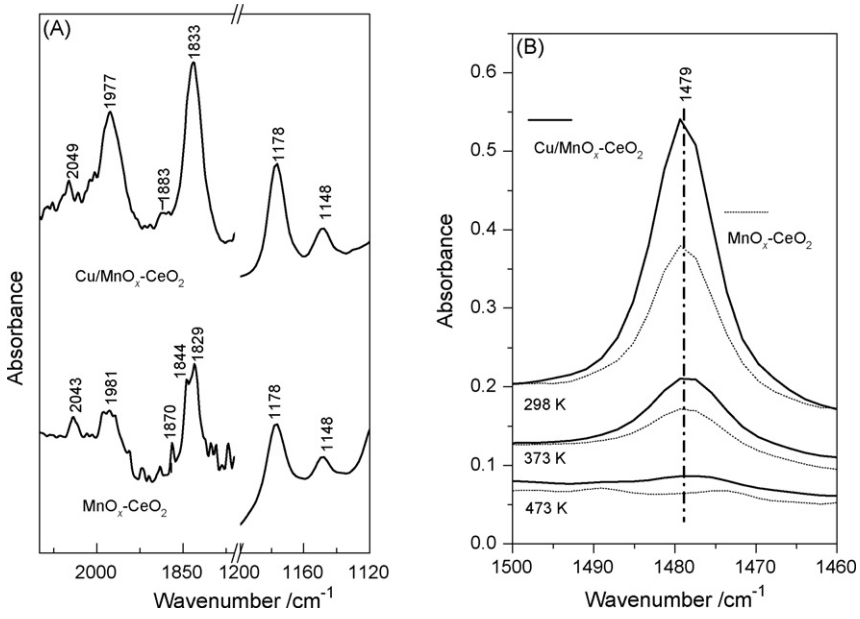

Fig. 5. FTIR spectra of adsorbed benzene on the MnO_x–CeO_2 support and the Cu/MnO_x–CeO_2 catalyst.

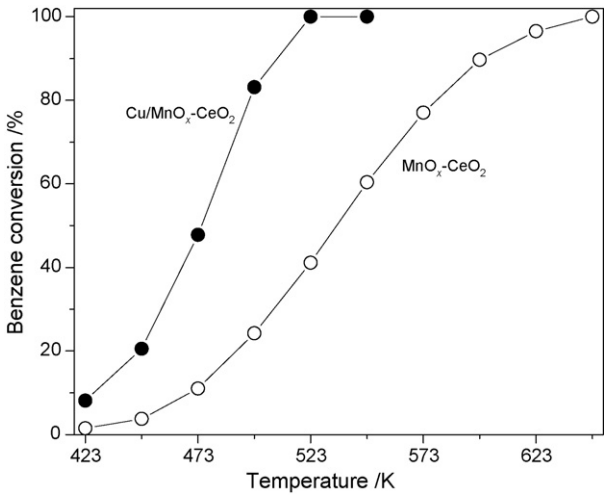

Fig. 6. Temperature dependence of the benzene conversions over MnO_x–CeO_2 mixed oxide and Cu/MnO_x–CeO_2 catalyst. Sample = 200 mg, benzene = 200 ppm, O_2 = 20.0%, He balance, GHSV = 30,000 mL/(g_{cat} h).

benzene and probably benzene was mainly adsorbed on copper species.

3.3. Complete oxidation of benzene

Fig. 6 shows the benzene conversions over the MnO_x–CeO_2 support and the Cu/MnO_x–CeO_2 catalyst as a function of reaction temperature. Carbon dioxide and water were detected as the only products, and no carbon monoxide or other intermediates could be observed. Complete conversion of benzene to CO_2 and water was achieved over the MnO_x–CeO_2 mixed oxide at 648 K, while the addition of copper greatly improved the catalytic activities and significantly lowered the temperature required for the complete oxidation of benzene. The Cu/MnO_x–CeO_2 catalyst exhibited much higher catalytic activity in the whole temperature range, and 100% conversion of benzene to CO_2 and H_2O was obtained at 523 K. Fig. 7 compares the activation energies of benzene oxidation over the MnO_x–CeO_2 mixed oxide and the Cu/MnO_x–CeO_2 catalyst. Obviously, the addition of copper to the MnO_x–CeO_2 mixed oxide caused the apparent activation energy decrease from 60.5 to 51.7 kJ/mol, and thus the enhanced catalytic activity was observed.

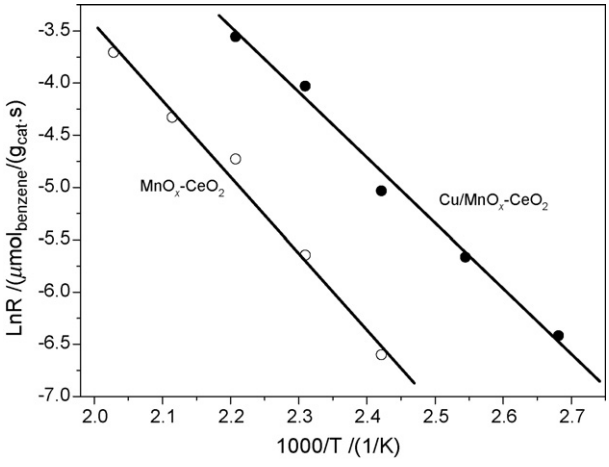

Fig. 7. Arrhenius diagrams of the reaction rates of benzene oxidation over MnO_x–CeO_2 mixed oxide and Cu/MnO_x–CeO_2 catalyst. Sample = 100 mg, benzene = 200 ppm, O_2 = 20.0%, He balance, GHSV = 30,000 mL/(g_{cat} h).

The complete oxidation of benzene even at 523 K demonstrated that the Cu/MnO_x–CeO_2 catalyst possessed high catalytic activity similar to supported noble metal catalysts [1–5] and much better than the Cu catalysts [10,11]. This can be attributed to the promoting effect of copper addition to the MnO_x–CeO_2 mixed oxide through the effective metal-support interaction. The metal-support interaction might be interpreted by the redox mechanism: the oxygen species released from the decomposition of CuO participated in the oxidation of adsorbed benzene, and the re-oxidation of reduced copper species (Cu_2O and/or Cu) to CuO would be achieved through the oxygen species from MnO_x–CeO_2 (MnO_x and/or CeO_2) in their vicinity [13,14]. The manganese and cerium species with the low oxidation state can be reoxidized by the gas-phase oxygen in the feed stream. The H_2-TPR measurements clearly indicated that addition of copper to MnO_x–CeO_2 support greatly prompted the reducibility of the Cu/MnO_x–CeO_2 catalyst, and thus facilitated the activation of oxygen molecule on the surface. Generally, rich defective oxygen species (O_β species) on the surface of the catalysts lead to higher catalytic activities [22]. Thus, the remarkable increase of O_β species observed by XPS measurement after the addition of copper species might play an important role in promoting the catalytic activities. Simultaneously, the FTIR study further revealed that the addition of copper not only provided more active sites for benzene adsorption, but also enhanced the absorption ability of benzene.

4. Conclusions

Addition of copper significantly improved the catalytic activity of MnO_x–CeO_2 mixed oxide for complete oxidation of benzene. Complete conversion of benzene was achieved at a temperature as low as 525 K over the Cu/MnO_x–CeO_2 catalyst. XRD and H_2-TPR measurements revealed that the copper species were highly dispersed on the surface of the mixed oxide, which promoted the reduction ability of the catalyst. Surface analysis by XPS and FTIR of absorbed benzene indicated that the increased O_β species and the created active sites for benzene adsorption simultaneously promoted the catalytic activity of the Cu/MnO_x–CeO_2 catalyst for the complete oxidation of benzene.

References

[1] L. Becker, H. Förster, Appl. Catal. B 17 (1998) 43–49.
[2] R.S.G. Ferreira, P.G.P. de Oliveira, F.B. Noronha, Appl. Catal. B 50 (2004) 243–249.
[3] H. Kim, T. Kim, H. Koh, S. Lee, B. Min, Appl. Catal. A 280 (2005) 125–131.
[4] J. Li, X. Xu, Z. Jiang, Z. Hao, C. Hu, Environ. Sci. Technol. 39 (2005) 1319–1323.
[5] T. Garcia, B. Solsona, D. Cazorla-Amoro's, A. Linares-Solano, S.H. Taylor, Appl. Catal. B 62 (2006) 66–76.
[6] P. Papaefthimiou, T. Ioannides, X.E. Verykios, Appl. Catal. B 15 (1998) 75–92.
[7] D. Andreeva, R. Nedyalkova, L. Ilieva, M.V. Abrashev, Appl. Catal. B 52 (2004) 157–165.

[8] D. Andreeva, R. Nedyalkova, L. Ilieva, M.V. Abrashev, Appl. Catal. A 246 (2003) 29–38.
[9] M.A. Centeno, M. Paulis, M. Montes, J.A. Odriozola, Appl. Catal. A 234 (2002) 65–78.
[10] S.C. Kim, J. Hazard. Mater. 91 (2002) 285–299.
[11] C. Wang, S. Lin, C. Chen, H. Weng, Chemosphere 64 (2006) 503–509.
[12] A. Tschöe, W. Liu, M. Flytzani-Stephanopoulos, J.Y. Ying, J. Catal. 157 (1995) 42–50.
[13] G. Sedmak, St. Hočevar, J. Levec, J. Catal. 213 (2003) 135–150.
[14] S. Hočevar, U.O. Krašvec, B. Orel, A.S. Aricó, H. Kim, Appl. Catal. B 8 (2000) 113–125.
[15] A. Pintar, J. Batista, S. Hočevar, J. Colloid Interface. Sci. 285 (2005) 218–231.
[16] G. Qi, R.T. Yang, R. Chang, Appl. Catal. B 51 (2004) 93–106.
[17] G. Qi, R.T. Yang, J. Catal. 217 (2003) 434–441.
[18] X. Tang, Y. Li, X. Huang, Y. Xu, H. Zhu, J. Wang, W. Shen, Appl. Catal. B 62 (2006) 265–273.
[19] H.P. Klug, L.E. Alexander, X-Ray Diffraction Procedures, John Wiley, New York, 1954.
[20] M. Machida, M. Uto, D. Kurogi, T. Kijima, Chem. Mater. 12 (2000) 3158–3164.
[21] A. Trovarelli, Catal. Rev. Sci. Eng. 38 (1996) 439–520.
[22] X. Tang, B. Zhang, Y. Li, Y. Xu, Q. Xin, W. Shen, Appl. Catal. A 288 (2005) 116–125.
[23] A. Bensalem, F. Bozon-Verduraz, M. Delamar, G. Bugli, Appl. Catal. A 121 (1995) 81–93.
[24] S. Hamoudi, F. Larachi, A. Adnot, A. Sayari, J. Catal. 185 (1999) 333–344.
[25] J.P. Holgado, G. Munuera, J.P. Espinós, A.R. González-Elipe, Appl. Surf. Sci. 158 (2000) 164–171.
[26] F. Larachi, J. Pierre, A. Adnot, A. Bernis, Appl. Surf. Sci. 195 (2002) 236–250.
[27] V.D. Castro, C. Furlani, Appl. Surf. Sci. 28 (1987) 270–278.
[28] B.L. Su, V. Norberg, J.A. Martens, Langmuir 17 (2001) 1267–1276.
[29] B.L. Su, D. Barthomeuf, J. Catal. 139 (2001) 81–92.